



ELSEVIER

Journal of Magnetism and Magnetic Materials 182 (1998) 369–374

M Journal of
M magnetism
M and
magnetic
materials

Electronic structure and magnetic properties of δ -MnGa

Zongxian Yang^{a,*}, Jun Li^b, Ding-sheng Wang^b, Kaiming Zhang^a, Xide Xie^a

^aSurface Physics Laboratory, Department of Physics, Fudan University, Shanghai 200433, China

^bLaboratory for Surface Physics, Institute of Physics and Center for Condensed Matter Physics, Academia Sinica, Beijing 100080, China

Received 7 August 1997

Abstract

The electronic structure and magnetic properties of δ -MnGa are studied by using the self-consistent linearized augmented plane-wave (LAPW) method. The analyses from the band structure, the density of states, total energy and the magnetic moments show that the ground states of the unstrained and strained δ -MnGa are in ferromagnetic phases, and the magnetic structures are affected significantly by strain. © 1998 Elsevier Science B.V. All rights reserved.

PACS: 75.50. – y

Keywords: Electronic structure; Magnetic properties; Linearized augmented plane-wave method

1. Introduction

One of the most attractive new directions both for material science and for device applications is the integration of magnetic materials and III–V semiconductors, which may offer possibilities of hybrid ferromagnetic-semiconductor devices. Recently, ferromagnetic MnGa ultrathin films and MnGa/NiGa magnetic multilayers have been successfully grown on GaAs substrates by molecular beam epitaxy [1–3]. It is found that the monocrystalline MnGa films are grown with the *c*-axis of the tetragonal unit cell normal to the (0 0 1)GaAs sub-

strates. The ferromagnetic MnGa films have excellent magnetic properties, such as square-hysteresis characteristics for applied fields perpendicular to the substrate, showing that this material could be a promising candidate which might closely integrate nonvolatile magnetic memory with the high-speed semiconductor circuitry.

Very recently, Shi et al. [4,5] reported that sub-micron MnGa ferromagnets with controllable magnetic properties had been successfully incorporated into GaAs semiconductors by Mn⁺ ion implantation and subsequent heat treatment. Such materials would offer great potential for studying carrier-spin scattering since the carrier densities can be tunable over a wide range and their spatial confinement easily controlled. These systems may be good candidates for new magnetoelectronic and magneto-optical devices.

* Corresponding author. Fax: +86 21 6549 3232; e-mail: 960033@fudan.edu.cn.

These examples reveal that MnGa is an interesting material with many potential applications. Therefore, it is worthwhile to perform a systematic study on this system. Experimentally, the crystal structure and magnetic properties of the $\text{Mn}_x\text{Ga}_{1-x}$ system had been studied by Hasegawa et al. [6] and Lu et al. [7,8]. It was found that there exist more than 10 different phases in the entire $\text{Mn}_x\text{Ga}_{1-x}$ system. Among these phases, five of them are ferromagnetic. The most pronounced ferromagnetic phase is the δ -MnGa which has a body centered tetragonal crystal structure with CuAu-I type ordering. The ideal stoichiometric composition ratio for Mn : Ga is 1 : 1, i.e., each unit cell consists of one manganese and one gallium atom occupying the (0 0 0) and $(\frac{1}{2} \frac{1}{2} \frac{1}{2})$ sites, respectively. δ -MnGa is stable at room temperature with the lattice parameters $a = 2.74 \text{ \AA}$ and $c = 3.69\text{--}3.58 \text{ \AA}$ for Mn content of 54.5–70 at% [6–8].

To our knowledge, no theoretical band studies have been performed on this material. In this paper, the electronic structure and magnetic properties of the δ -MnGa are studied using the self-consistent linearized augmented plane-wave (LAPW) method. The strain effects on the electronic and magnetic structure corresponding to the cases of δ -MnGa films grown on GaAs(0 0 1) and δ -MnGa/NiGa superlattices on GaAs(0 0 1) are also considered. The ideal stoichiometric composition for the δ -MnGa is adopted for simplicity. The organization of the paper is as follows: in Section 2 we briefly give the details of the theoretical method; the results and discussion are presented in Section 3 and a brief summary is presented in Section 4.

2. Model and calculation method

In this paper, the self-consistent linearized augmented plane-wave (LAPW) method [9–11] with the von Barth–Hedin exchange-correlation term is used to carry out the calculation of the electronic structure and magnetic properties. Only the *ideal* stoichiometric composition for the δ -MnGa, i.e., a crystallographic tetragonal lattice unit cell consisting of one Mn atom at (0 0 0) and one Ga at $(\frac{1}{2} \frac{1}{2} \frac{1}{2})$ is adopted for simplicity in present calculation. In order to achieve a better understanding of

the electronic structure and magnetic properties for the cases of δ -MnGa films grown on GaAs(0 0 1) and δ -MnGa/NiGa superlattices grown on GaAs(0 0 1), strain effects are also considered. The basis size used in solving the eigenvalue problem is about 50 LAPWs per atom, and the self-consistent calculations were carried out by using 40 special k points in the irreducible wedge of the first Brillouin zone of the tetragonal unit cell. Calculations show that the results using 75 special k points have only slight quantitative difference. The convergence measured by the rms difference between input and output is better than 0.01 me/a.u.^3 for the charge density and for the spin density. The total energy is converged to better than 0.02 mRy .

3. Results and discussion

3.1. Unstrained ideal δ -MnGa system

For the unstrained ideal δ -MnGa system, a tetragonal unit cell with lattice parameters $a = 2.74 \text{ \AA}$ and $c = 3.69 \text{ \AA}$ is adopted in the calculation [6–8]. It is found that the ground state for this system is ferromagnetic (FM) with the total energy of 0.53 eV lower than the corresponding paramagnetic (PM) state. The magnetic moments are $2.51 \mu_B$ per Mn atom and $-0.11 \mu_B$ per Ga atom (the minus sign represents that the magnetic moment of Ga is anti-parallel to that of Mn), which are given by the integration over Mn and Ga muffin-tin sphere region with radius equal to 1.28 and 1.37 \AA , respectively.

The calculated band structure for the PM and FM phases which are plotted by simply connecting the eigenvalues in energy sequence are shown in Figs. 1 and 2, respectively. By comparing with the bands of the PM phase, it is found that the spin-up and -down bands of the FM phase show similar dispersion, with the spin-up bands shift towards higher binding energy against the spin-down bands. The exchange splitting is obvious, however, it is not the same for all bands and all k points. It is found that bands near the Fermi energy have large exchange splitting.

In Figs. 3 and 4 we present the total density of states (TDOS) of the unit cell and the local density

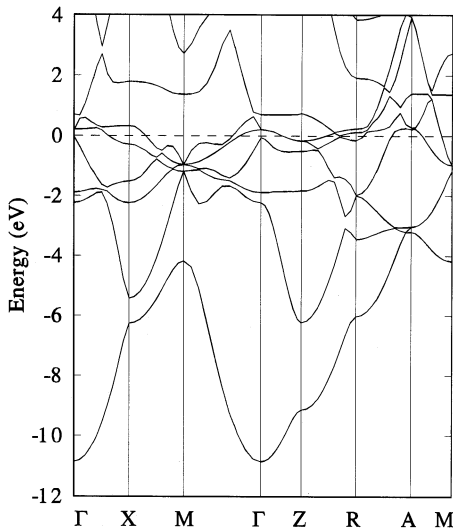


Fig. 1. Band structure for the PM phase of the unstrained ideal stoichiometric bulk δ -MnGa. Energies are measured relative to the Fermi level.

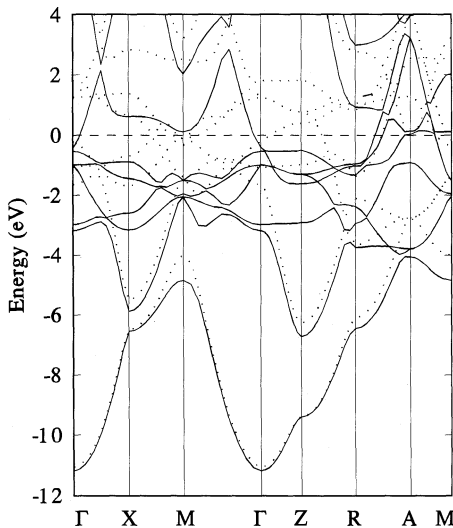


Fig. 2. Band structure for the FM phase of the unstrained ideal stoichiometric bulk δ -MnGa. The solid lines indicate majority (up) spin and the dotted lines indicate minority (down) spin. Energies are measured relative to the Fermi level.

of states (LDOS) of Mn atom, respectively. When the magnetic configuration is changed from the PM to the FM phase, similar to other ferromagnets, the

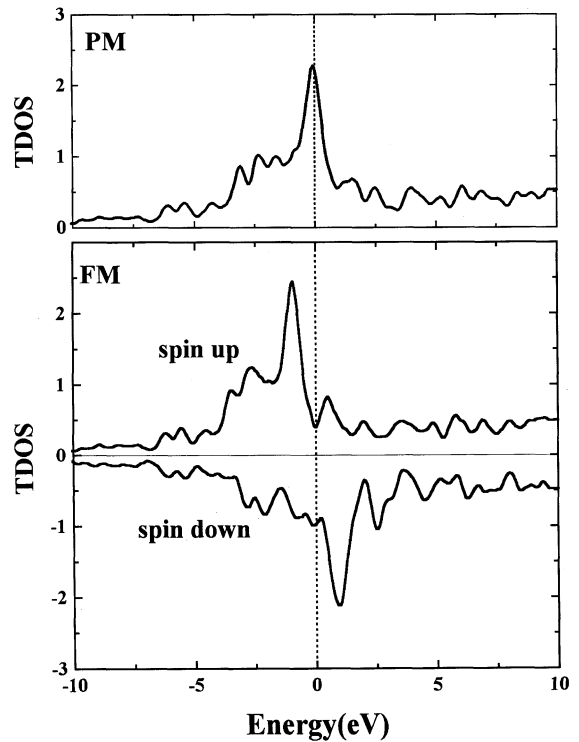


Fig. 3. Total density of states (TDOS) of the unit cell for the PM and FM phases in $1/\text{eV} \cdot \text{spin}$. The vertical dotted line denotes the Fermi level.

width of the majority band is narrower than the minority band since the minority electrons are in less strong bonding and thus have stronger interaction among themselves. The local density of states of the Mn atom shown in Fig. 4 has the similar features. The further analysis of the Mn local density of states reveals that the magnetic structure is governed by the Mn 3d states, which lead to the peak structures in total density of states in addition to the background coming from the Mn 4s and Ga 4s, 4p electrons as shown in Fig. 3.

3.2. Strained δ -MnGa system

Experimental results [1–3] have shown that the MnGa films grown on GaAs(001) substrate or in the MnGa/NiGa superlattices (which is also grown on GaAs(001) substrate) have reduced tetragonality, with c values of 3.1 or 3.5 Å, respectively. This reduced tetragonality influences the magnetic

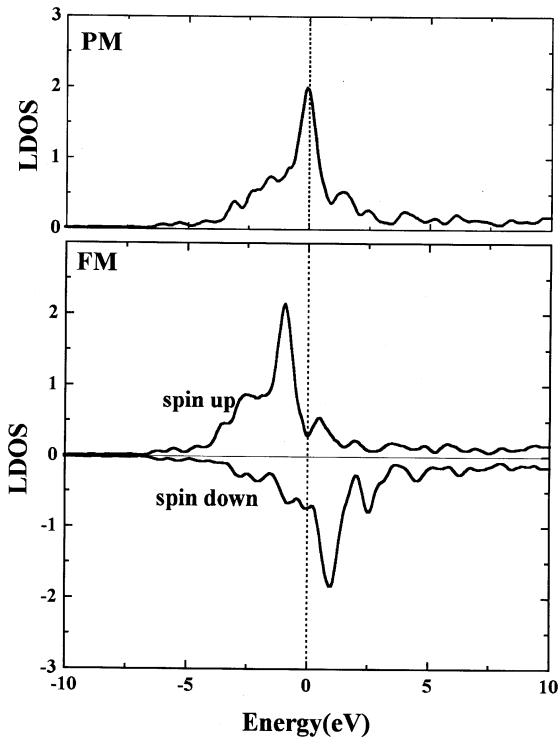


Fig. 4. Local density of states (LDOS) of Mn atom for the PM and FM phases. The vertical dotted line denotes the Fermi level.

properties, particularly the coercive field of the ferromagnetic films [1–3]. This is attributed to the lattice strain, since for bulk crystals the lattice constant a of the tetragonal MnGa and CsCl-type NiGa are 2.74 and 2.89 Å, which have the lattice mismatch of -3.2% and $+2.1\%$ with half of the lattice constant of the substrate GaAs(0 0 1), 2.83 Å, respectively. Therefore, it is necessary to consider the lattice strain to simulate the cases of the MnGa films on GaAs(0 0 1) substrate and in the MnGa/NiGa superlattices.

Since there are no experimental elastic constants available for the MnGa system, we try to include the strain effects in the following way. Considering that both the MnGa films and the MnGa/NiGa superlattices are grown on GaAs(0 0 1) substrates, we choose a tetragonal lattice unit cell with its basal plane constant a fixed at 2.83 Å (half of the lattice constant of GaAs) and with the value of c varying from 3.0 to 3.7 Å in a step of 0.1 Å, which covers the

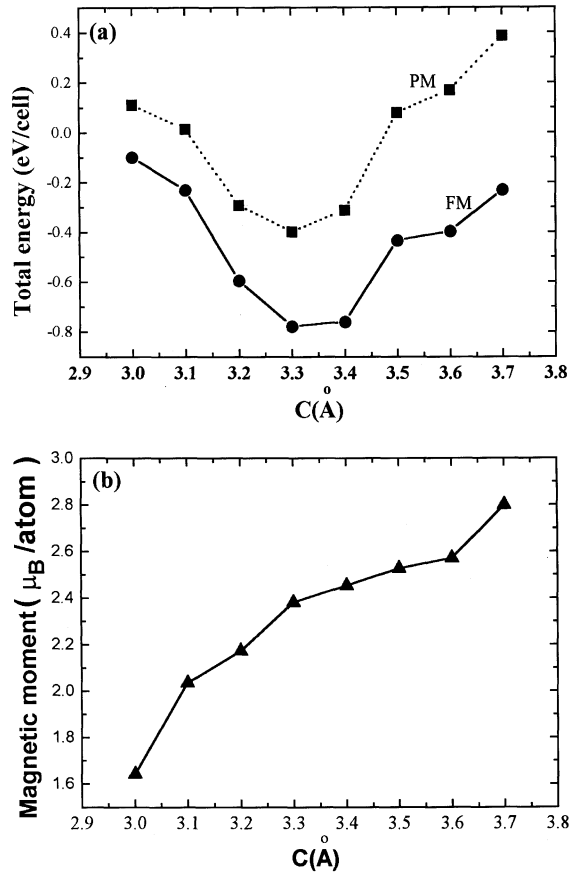


Fig. 5. (a) total energy (relative to that of PM phase of the unstrained δ -MnGa) versus c values of the strained unit cell for the PM phase (solid squares connected by dotted lines) and FM phase (solid circles connected by solid lines). (b) magnetic moments per Mn atom versus c values of the strained δ -MnGa for the FM phase.

case of MnGa films on GaAs(0 0 1) (3.1 Å) and that of MnGa/NiGa superlattices (3.5 Å). The self-consistent calculation was performed to determine the total energy for each step. The most possible c value should correspond to the one which gives the lowest total energy.

The calculated results are shown in Fig. 5a and Fig. 5b. In Fig. 5a, the unit cell total energy (relative to the total energy of the PM unstrained ideal δ -MnGa phase) versus the c values for the PM phase and FM phase is plotted in solid squares (dotted line) and in solid circles (solid line), respectively. It is found that, in the whole range of c values

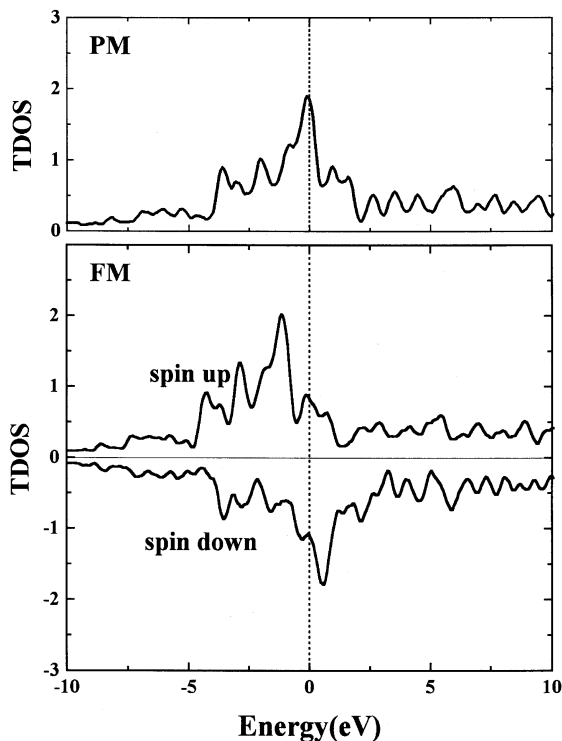


Fig. 6. Total density of states (TDOS) of PM and FM phases for the strained unit cell with $a = 2.83 \text{ \AA}$ and $c = 3.1 \text{ \AA}$. The vertical dotted line denotes the Fermi level.

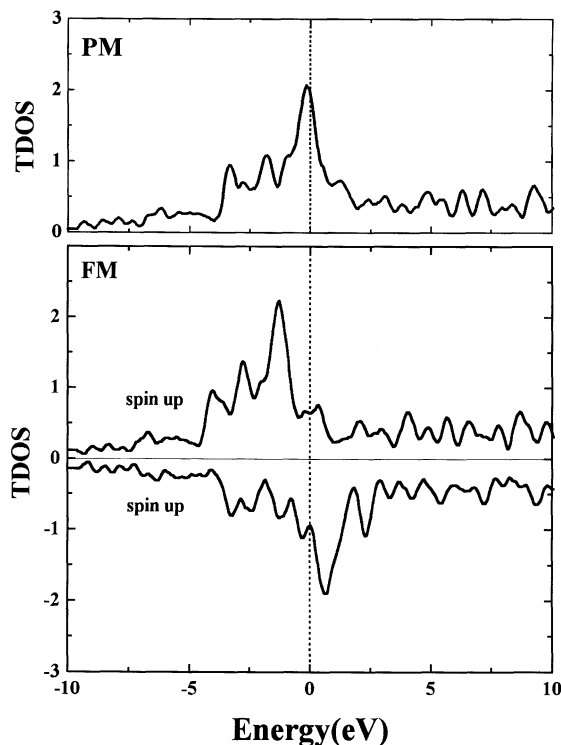


Fig. 7. Total density of states (TDOS) of PM and FM phases for the strained unit cell with $a = 2.83 \text{ \AA}$ and $c = 3.3 \text{ \AA}$. The vertical dotted line denotes the Fermi level.

considered, the total energy of the FM phases is lower than that of their corresponding PM phases. The lowest total energy corresponds to c value of 3.3 \AA , which is in the middle of 3.1 \AA for the case of $\delta\text{-MnGa}$ on $\text{GaAs}(001)$ and 3.5 \AA for the case of the superlattices grown on $\text{GaAs}(001)$. From Fig. 5b it is found that, in the FM phases, the magnetic moment per Mn atom increases with the increase of c . It was also shown from the calculated results that the magnetic moment of Ga is always antiparallel to that of Mn, and less than $0.11 \mu_B$ per Ga atom (which are not plotted in the figures). For the three particular c values of 3.1 , 3.5 and 3.3 \AA related to the experimental values and the optimal value determined by our total energy calculation, the magnetic moments per Mn atom are 2.04 , 2.53 and $2.33 \mu_B$, respectively. Comparing to the magnetic moments per Mn atom of the unstrained ideal $\delta\text{-MnGa}$, it can be concluded that strain has large effect on the magnetic properties.

In order to have a better understanding for the strain effects, we present also the total density of states of PM and FM phases for three particular cases which correspond to the c values of 3.1 , 3.3 and 3.5 \AA , respectively. The basal plane constant a is fixed at 2.83 \AA . The results are shown in Figs. 6–8. From the TDOS curves for the PM phases for the three cases, it can be seen that the increase of c values results in narrower and larger density of states around the Fermi energy. This is the consequence of the decrease of the interatomic hybridization. According to the Stoner criterion [12] for ferromagnetism, $I \times N(E_F) \geq 1$, where the exchange integral (Stoner parameter) I is related to the exchange-correlation functional and is approximately structure independent, the increase in $N(E_F)$, the density of states at the Fermi energy, will enhance the tendency towards ferromagnetism. Therefore, the increase of the magnetic moments with c value is easily understood. The TDOS curves

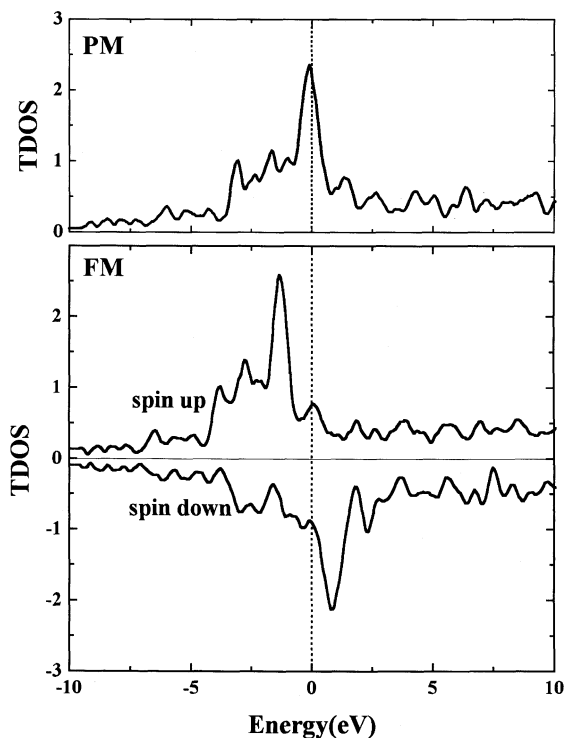


Fig. 8. Total density of states (TDOS) of PM and FM phases for the strained unit cell with $a = 2.83 \text{ \AA}$ and $c = 3.5 \text{ \AA}$. The vertical dotted line denotes the Fermi level.

of Figs. 6–8 for the FM phases also show the narrowing and increasing of the majority density peaks with the increase of c value. The exchange splitting also increase with the c value in accordance with the enhancement of the tendency towards ferromagnetism.

4. Summary

In summary, the electronic and magnetic structures of the unstrained and strained of stoichiometric δ -MnGa are studied using the self-consistent linearized augmented plane-wave (LAPW) method. The analyses from the band structure, the density of states and the magnetic moments show that the

ground states of the unstrained and strained δ -MnGa are in ferromagnetic phases. When the basal plane constant is adopted as 2.83 \AA (half of the lattice constant of GaAs), the optimal c value for the strained unit cell determined by the total energy calculation is 3.3 \AA , the magnetic moments per Mn atom is $2.33 \mu_B$, which is smaller than that of unstrained case. It is also found that the magnetic structures are governed by the Mn 3d states and can be affected largely by strain.

Acknowledgements

One of the authors (Zongxian Yang) wishes to thank Prof. Yumei Zhou, Mr. Wen-tong Geng and Mr. Chun-gang Duan of the Institute of Physics, Chinese Academy of Sciences, for useful discussions.

References

- [1] M. Tanaka, J.P. Harbison, J. Deboeck, T. Sands, B. Philips, T.L. Cheeks, V.G. Keramidas, *Appl. Phys. Lett.* 62 (1993) 1565.
- [2] M. Tanaka, J.P. Harbison, T. Sands, B. Philips, T.L. Cheeks, J. Deboeck, L.T. Florez, V.G. Keramidas, *Appl. Phys. Lett.* 63 (1993) 696.
- [3] M. Tanaka, *Mater. Sci. Eng. B* 31 (1995) 117.
- [4] Jing Shi, S. Gider, K. Babcock, D.D. Awschalm, *Science* 271 (1996) 937.
- [5] Jing Shi, J.M. Kikkawa, D.D. Awschalm, G. Medeiros-Ribeiro, P.M. Petroff, K. Babcock, *J. Appl. Phys.* 79 (1996) 5296.
- [6] M. Hasegawa, I. Tsuboya, *Rev. Electrical Commun. Lab.* 16 (1968) 605.
- [7] Xue-shan Lu, Jing-kui Liang, Zhong-ruo Yang, *Acta Phys. Sin.* 28 (1979) 54.
- [8] Xue-shan Lu, Jing-kui Liang, Ting-jun Shi, Min-qiang Zhou, *Acta Phys. Sin.* 29 (1980) 469.
- [9] D.D. Koelling, G.O. Arbman, *J. Phys. F* 5 (1975) 2041.
- [10] H. Krakauer, M. Posternak, A.J. Freeman, *Phys. Rev. B* 19 (1979) 1706.
- [11] M. Posternak, H. Krakauer, A.J. Freeman, D.D. Koelling, *Phys. Rev. B* 21 (1980) 5601.
- [12] J. Kübler, V. Eyert, in: R.W. Cahn, P. Haasen, E.J. Kramer (Eds.), *Materials Science and Technology*, vol. 3A, VCH, Weinheim, p. 102.